Proceedings of the 2007 American Control Conference
Marriott Marquis Hotel at Times Square
New York City, USA, July 11-13, 2007



# Duhem Feedback and Friction-Induced Staircase Hysteresis*

Ashwani K. Padthe† and Dennis S. Bernstein†

†Department of Aerospace Engineering, The University of Michigan,
Ann Arbor, MI 48109-2140, USA, {akpadthe,dsbaero}@umich.edu

*Abstract*— **In this paper we provide a system-theoretic picture of the hysteresis induced by friction. We study the hysteretic response of a linear system connected with a Duhem hysteretic model in the feedback. We then use the popular Dahl and LuGre Duhem friction models to model the mass-spring system with friction, as a linear system with Duhem feedback. We use the feedback model to study the hysteretic response between the external force applied on the mass and the displacement of the mass.**

## I. Introduction

Modeling and control of friction remains a problem of interest, both for its intellectual challenge and its practical ramifications [1]–[8]. In recent work [9] we considered the relationship between friction models and hysteresis in mechanical systems. In particular, by using the results in [10] on Duhem models for hysteresis, we classified several popular friction models in terms of the properties of the relevant Duhem model; see Table I.

In [11] we developed an experimental testbed for friction identification. The testbed consists of a dc motor with a speed reduction gearhead, with encoder measurements of the shaft and load cell measurements of a cable wound around the gearhead. By operating this testbed under quasi static conditions, we compared its hysteretic response to the simulated response of the system under various friction models. The LuGre friction model, which exhibits stick-slip friction, was found to provide the best model of the testbed's hysteretic dynamics.

In the present paper we provide a broader, system-theoretic picture of the hysteresis induced by friction. Using the classifications in [9], we model SDOF dynamics with friction force as a linear system with Duhem hysteretic feedback and study the input-output hysteretic map of the closed-loop system. In particular, we examine the relationship between the equilibria map and the hysteretic map of the closed-loop. While friction is known to be a source of hysteresis [6], [7], [11], [12], our goal is to systematically examine the link between the physical phenomenon of friction and the system-theoretic phenomenon of hysteresis.

In Section 2 we review the basic theory of the Duhem model from [10]. In Section 3 we review the analysis from [9] of the Dahl and LuGre friction models concerning their hysteretic characteristics. In Section 4 we study the hysteretic response of a linear system under Duhem feedback. Then, we model a mass-spring system with friction as a linear system with a Duhem feedback and characterize the hysteretic map between the force actuation and the position output. We carry out this analysis with both the friction models. In Section 5 we give some concluding remarks.

*This research was supported in part by the National Science Foundation under grant ECS–0225799.

## II. Generalized and Semilinear Duhem Models

In this section, we summarize the main results of [10] concerning the generalized and semilinear Duhem models. Consider the single-input single-output *generalized Duhem model*

$$\dot{x}(t) = f\big(x(t), u(t)\big)g\big(\dot{u}(t)\big), \qquad x(0) = x_0, \quad t \geq 0, \tag{1}$$

$$y(t) = h\big(x(t), u(t)\big), \tag{2}$$

where $x : [0, \infty) \to \mathbb{R}^n$ is absolutely continuous, $u : [0, \infty) \to \mathbb{R}$ is continuous and piecewise $\mathrm{C}^1$, $f : \mathbb{R}^n \times \mathbb{R} \to \mathbb{R}^{n\times r}$ is continuous, $g : \mathbb{R} \to \mathbb{R}^r$ is continuous and satisfies $g(0) = 0$, and $y : [0, \infty) \to \mathbb{R}$, and $h : \mathbb{R}^n \times \mathbb{R} \to \mathbb{R}$ are continuous. The value of $\dot{x}(t)$ at a point $t$ at which $\dot{u}(t)$ does not exist can be assigned arbitrarily. We assume that the solution to (1) exists and is unique on all finite intervals. Under these assumptions, $x$ and $y$ are continuous and piecewise $\mathrm{C}^1$. The terms closed curve, limiting periodic input-output map, hysteresis map, and rate independence are defined as follows.

*Definition 2.1:* The nonempty set $\mathcal{H} \subset \mathbb{R}^2$ is a *closed curve* if there exists a continuous, piecewise $\mathrm{C}^1$, and periodic map $\delta : [0, \infty) \to \mathbb{R}^2$ such that $\delta([0, \infty)) = \mathcal{H}$.

| Friction Model | | Duhem Type | Rate Dependence | Continuity |
|---|---|---|---|---|
| Coulomb | | static | rate independent | discontinuous |
| Dahl | $\gamma = 0$ | generalized | rate independent | discontinuous |
| | $0 < \gamma < 1$ | generalized | rate independent | continuous but not Lipschitz |
| | $\gamma = 1$ | semilinear | rate independent | Lipschitz |
| | $\gamma > 1$ | generalized | rate independent | Lipschitz |
| LuGre | | generalized | rate dependent | Lipschitz |

TABLE I

Classification and properties of friction models. Each friction model is a Duhem model, with either rate-independent or rate-dependent dynamics. Non-Lipschitzian dynamics is a necessary condition for finite-time convergence, which reflects nonunique behavior in reverse time.

*Definition 2.2:* Let $u : [0,\infty] \to [u_{\min}, u_{\max}]$ be continuous, piecewise $C^1$, periodic with period $\alpha$, and have exactly one local maximum $u_{\max}$ in $[0,\alpha)$ and exactly one local minimum $u_{\min}$ in $[0,\alpha)$. For all $T > 0$, define $u_T(t) \triangleq u(\alpha t/T)$, assume that there exists $x_T : [0,\infty) \to \mathbb{R}^n$ that is periodic with period $T$ and satisfies (1) with $u = u_T$, and let $y_T : [0,\infty) \to \mathbb{R}$ be given by (2) with $x = x_T$ and $u = u_T$. For all $T > 0$, the *periodic input-output map* $\mathcal{H}_T(u_T, y_T)$ is the closed curve $\mathcal{H}_T(u_T, y_T) \triangleq \{(u_T(t), y_T(t)) : t \in [0,\infty)\}$, and the *limiting periodic input-output map* $\mathcal{H}_\infty(u)$ is the closed curve $\mathcal{H}_\infty(u) \triangleq \lim_{T\to\infty} \mathcal{H}_T(u_T, y_T)$ if the limit exists. If there exist $(u, y_1), (u, y_2) \in \mathcal{H}_\infty(u)$ such that $y_1 \neq y_2$, then $\mathcal{H}_\infty(u)$ is a *hysteresis map*, and the generalized Duhem model is *hysteretic*.

*Definition 2.3:* The continuous and piecewise $C^1$ function $\tau : [0,\infty) \to [0,\infty)$ is a *positive time scale* if $\tau(0) = 0$, $\tau$ is nondecreasing, and $\lim_{t\to\infty} \tau(t) = \infty$. The generalized Duhem model (1), (2) is *rate independent* if, for every pair of continuous and piecewise $C^1$ functions $x$ and $u$ satisfying (1) and for every positive time scale $\tau$, it follows that $x_\tau(t) \triangleq x(\tau(t))$ and $u_\tau(t) \triangleq u(\tau(t))$ also satisfy (1).

The following result is proved in [10].

*Proposition 2.1:* Assume that $g$ is positively homogeneous, that is, $g(\alpha v) = \alpha g(v)$ for all $\alpha > 0$ and $v \in \mathbb{R}$. Then the generalized Duhem model (1), (2) is rate independent.

If $g$ is positively homogeneous, then there exist $h_+, h_- \in \mathbb{R}^r$ such that

$$g(v) = \begin{cases} h_+ v, & v \geq 0, \\ h_- v, & v < 0, \end{cases} \tag{3}$$

and the rate-independent generalized Duhem model (1), (2) can be reparameterized in terms of $u$ [10]. Specifically, consider

$$\frac{\mathrm{d}\hat{x}(u)}{\mathrm{d}u} = \begin{cases} f_+(\hat{x}(u), u), & \text{when } u \text{ increases}, \\ f_-(\hat{x}(u), u), & \text{when } u \text{ decreases}, \\ 0, & \text{otherwise}, \end{cases} \tag{4}$$

$$\hat{y}(u) = h\big(\hat{x}(u), u\big), \tag{5}$$

for $u \in [u_{\min}, u_{\max}]$ and with initial condition $\hat{x}(u_0) = x_0$, where $f_+(x,u) \triangleq f(x,u)h_+$, $f_-(x,u) \triangleq f(x,u)h_-$, and $u_0 \in [u_{\min}, u_{\max}]$. Then $x(t) \triangleq \hat{x}(u(t))$ and $y(t) \triangleq \hat{y}(u(t))$ satisfy (1), (2). Note that the reparameterized Duhem model (4) and (5) can be viewed as a time-varying dynamical system with nonmonotonic time $u$.

As a specialization of (1) and (2), we now consider the *rate-independent semilinear Duhem model*

$$\dot{x}(t) = \begin{bmatrix} \dot{u}_+(t) I_n & \dot{u}_-(t) I_n \end{bmatrix} \times \left( \begin{bmatrix} A_+ \\ A_- \end{bmatrix} x(t) + \begin{bmatrix} B_+ \\ B_- \end{bmatrix} u(t) + \begin{bmatrix} E_+ \\ E_- \end{bmatrix} \right), \tag{6}$$

$$y(t) = Cx(t) + Du(t), \qquad x(0) = x_0, \quad t \geq 0, \tag{7}$$

where $A_+ \in \mathbb{R}^{n\times n}$, $A_- \in \mathbb{R}^{n\times n}$, $B_+ \in \mathbb{R}^n$, $B_- \in \mathbb{R}^n$, $E_+ \in \mathbb{R}^n$, $E_- \in \mathbb{R}^n$, $C \in \mathbb{R}^{1\times n}$, $D \in \mathbb{R}$, and

$$\dot{u}_+(t) \triangleq \max\{0, \dot{u}(t)\}, \quad \dot{u}_-(t) \triangleq \min\{0, \dot{u}(t)\}. \tag{8}$$

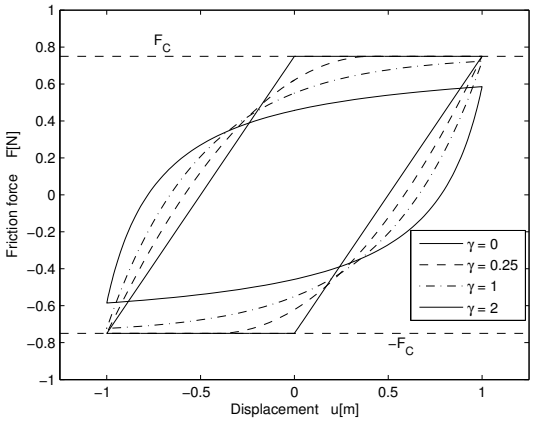


Fig. 1. Displacement $u$ versus the friction force $F$ for the Dahl model for several values of $\gamma$. The shape of the hysteresis loop between $F$ and $u$ is determined by the value of $\gamma$. The numerical values used are $F_C = 0.75$ N, $\sigma = 1.5$ N/m, and $u(t) = \sin 0.1t$ m.

Let $\rho(A)$ denote the spectral radius of $A \in \mathbb{R}^{n\times n}$ and let the *limiting input-output map* $\mathcal{F}_\infty(u,y)$ be the set of points $z \in \mathbb{R}^2$ such that there exists an increasing, divergent sequence $\{t_i\}_{i=1}^\infty$ in $[0,\infty)$ satisfying $\lim_{i\to\infty} \|(u(t_i), y(t_i)) - z\| = 0$. Theorem 4.1 in [10] provides a sufficient condition for the existence of the limiting periodic input-output map for a rate-independent semilinear Duhem model under the assumption

$$\rho\left(e^{\beta A_+} e^{-\beta A_-}\right) < 1. \tag{9}$$

## III. Friction Models

### A. Dahl model

The Dahl model [4] has the form

$$\dot{F}(t) = \sigma \left| 1 - \frac{F(t)}{F_C} \operatorname{sgn} \dot{u}(t) \right|^\gamma \operatorname{sgn}\left(1 - \frac{F(t)}{F_C} \operatorname{sgn} \dot{u}(t)\right) \dot{u}(t), \tag{10}$$

where $F$ is the friction force, $u$ is the relative displacement between the two surfaces in contact, $F_C > 0$ is the Coulomb friction force, $\gamma \geq 0$ is a parameter that determines the shape of the force-deflection curve (plot between the friction force and the relative displacement), and $\sigma > 0$ is the rest stiffness, that is, the slope of the force-deflection curve when $F = 0$. The right-hand side of (10) is Lipschitz continuous in $F$ for $\gamma \geq 1$ but not Lipschitz in $F$ for $0 \leq \gamma < 1$.

When $u$ is increasing, $\dot{F}(t)$ given by (10) is positive for all $F(t) < F_C$ and negative for all $F(t) > F_C$. Similarly, when $u$ is decreasing, $\dot{F}(t)$ given by (10) is positive for all $F(t) < -F_C$ and negative for all $F(t) > -F_C$. Hence the friction force $F(t)$ approaches $F_C$ under monotonic inputs. The parameter $\gamma$ determines the shape of the input-output map. The input-output hysteresis maps of the Dahl model for several values of $\gamma$ are shown in Figure 1. In practice, $\gamma$ is typically set to 0 or 1. The friction force given by the Dahl model lags the friction force given by the Coulomb model when the direction of motion is reversed.

To represent (10) as a Duhem model, let

$$\mathcal{F}_+\big(F\big) \triangleq \sigma \left|1 - \frac{F}{F_{\mathrm{C}}}\right|^{\gamma} \operatorname{sgn}\left(1 - \frac{F}{F_{\mathrm{C}}}\right), \tag{11}$$

$$\mathcal{F}_-\big(F\big) \triangleq \sigma \left|1 + \frac{F}{F_{\mathrm{C}}}\right|^{\gamma} \operatorname{sgn}\left(1 + \frac{F}{F_{\mathrm{C}}}\right). \tag{12}$$

Then the Dahl model (10) can be rewritten as

$$\dot{F}(t) = \sigma \begin{bmatrix} \mathcal{D}_+\big(F(t)\big) & \mathcal{D}_-\big(F(t)\big) \end{bmatrix} \begin{bmatrix} \dot{u}_+(t) \\ \dot{u}_-(t) \end{bmatrix}, \tag{13}$$

$$y = F \tag{14}$$

which for all $\gamma \geq 0$ is a generalized Duhem model of the form (1), (2). Furthermore, since $g(\dot{u}) = \begin{bmatrix} \dot{u}_+(t) & \dot{u}_-(t) \end{bmatrix}^{\mathrm{T}}$ is positively homogeneous, Proposition 2.1 implies that (13) is rate independent for all $\gamma \geq 0$.

Let $\gamma = 1$. Then (10) becomes

$$\begin{aligned} \dot{F}(t) &= \sigma \left(1 - \frac{F(t)}{F_{\mathrm{C}}} \operatorname{sgn} \dot{u}(t)\right) \dot{u}(t) \\ &= \begin{bmatrix} -\frac{\sigma}{F_{\mathrm{C}}} F(t) + \sigma & \frac{\sigma}{F_{\mathrm{C}}} F(t) + \sigma \end{bmatrix} \begin{bmatrix} \dot{u}_+(t) \\ \dot{u}_-(t) \end{bmatrix}, \end{aligned}$$

which is a rate-independent semilinear Duhem model. Furthermore, the convergence condition (9) becomes

$$e^{-2\frac{\beta\sigma}{F_{\mathrm{C}}}} < 1, \tag{15}$$

which holds if and only if $\beta > 0$. As a direct consequence of Theorem 4.1 in [10], which explicitly characterizes the hysteresis map, we have the following result. The corresponding hysteresis map is shown in Figure 1.

*Corollary 3.1:* Consider the Dahl model (10) with $\gamma = 1$. Let $u$ be continuous, piecewise $\mathrm{C}^1$, and periodic with period $\alpha$ and have exactly one local maximum $u_{\max}$ in $[0, \alpha)$ and exactly one local minimum $u_{\min}$ in $[0, \alpha)$. Then (15) holds, and (13), (14) has a unique periodic solution $F : [0, \infty) \to \mathbb{R}^n$, and the limiting periodic input-output map $\mathcal{H}_\infty(u)$ exists. Furthermore,

$$\begin{aligned} \mathcal{H}_\infty(u) = &\left\{\big(u, \hat{F}_+(u)\big) \in \mathbb{R}^2 : u \in [u_{\min}, u_{\max}]\right\} \\ &\cup \left\{\big(u, \hat{F}_-(u)\big) \in \mathbb{R}^2 : u \in [u_{\min}, u_{\max}]\right\}, \end{aligned} \tag{16}$$

where

$$\hat{F}_+(u) \triangleq e^{-\frac{\sigma}{F_{\mathrm{C}}}(u - u_{\min})} \hat{\alpha}_+ + F_{\mathrm{C}} \left(1 - e^{-\frac{\sigma}{F_{\mathrm{C}}}(u - u_{\min})}\right),$$

$$\hat{F}_-(u) \triangleq e^{\frac{\sigma}{F_{\mathrm{C}}}(u - u_{\max})} \hat{\alpha}_- - F_{\mathrm{C}} \left(1 - e^{-\frac{\sigma}{F_{\mathrm{C}}}(u - u_{\max})}\right),$$

and

$$\hat{\alpha}_+ = -\hat{\alpha}_- = F_{\mathrm{C}} \frac{e^{\frac{-\beta\sigma}{F_{\mathrm{C}}}} - 1}{e^{-\frac{\beta\sigma}{F_{\mathrm{C}}}} + 1}.$$

### B. LuGre Model

The LuGre model [5], which models the asperities of two surfaces as elastic bristles, is given by

$$\dot{x}(t) = \dot{u}(t) - \frac{|\dot{u}(t)|}{r\big(\dot{u}(t)\big)} x(t), \tag{17}$$

$$F(t) = \sigma_0 x(t) + \sigma_1 \dot{x}(t) + \sigma_2 \dot{u}(t), \tag{18}$$

where $x$ is the average deflection of the bristles, $u$ is the relative displacement, $F$ is the friction force, and $\sigma_0, \sigma_1, \sigma_2 > 0$ are stiffness, damping, and viscous friction coefficients, respectively. The right hand side of (17) is Lipschitz continuous in $x$. Various choices for the function $r(\dot{u}(t))$ are given in [1, p. 83].

For a given constant velocity $\dot{u}$, the steady-state friction force $F_{\mathrm{ss}}$ obtained from (17) and (18) is

$$F_{\mathrm{ss}}(\dot{u}) = \sigma_0 r(\dot{u}) \operatorname{sgn}(\dot{u}) + \sigma_2 \dot{u}. \tag{19}$$

The drop in friction force at low magnitudes of velocity is due to the Stribeck effect, while the Stribeck velocity is the velocity at which the steady-state friction force begins to decrease when the velocity is positive and increasing. The Lugre model (17), (18) combines the friction lag of the Dahl model with the Stribeck effect [5].

In [1], [5], $r(\dot{u}(t))$ is defined by

$$r(\dot{u}(t)) = \frac{F_{\mathrm{C}}}{\sigma_0} + \frac{F_{\mathrm{S}} - F_{\mathrm{C}}}{\sigma_0} e^{-(\dot{u}(t)/v_{\mathrm{S}})^2}, \tag{20}$$

where $F_{\mathrm{C}} > 0$ is the Coulomb friction force, $F_{\mathrm{S}}$ is the stiction (sticking friction) force, and $v_{\mathrm{S}}$ is the Stribeck velocity. Letting $F_{\mathrm{S}} = F_{\mathrm{C}}$ and $\sigma_1 = \sigma_2 = 0$ in (20), the LuGre model (17), (18), (20) is equivalent to the Dahl model (10) with $\gamma = 1$ and $\sigma = 1$. With $y = F$, the state equations (17) and (18) can be written as

$$\dot{x}(t) = \begin{bmatrix} 1 & x(t) \end{bmatrix} \begin{bmatrix} \dot{u}(t) \\ -\frac{|\dot{u}(t)|}{r\big(\dot{u}(t)\big)} \end{bmatrix}, \tag{21}$$

$$y(t) = \sigma_0 x(t) + \sigma_1 \dot{x}(t) + \sigma_2 \dot{u}(t), \tag{22}$$

which is a generalized Duhem model of the form (1). Since $r$ given in (20) is not a positively homogeneous function of $\dot{u}$, the LuGre model is not necessarily rate independent. In fact, the input-output maps in Figure 2 show that the LuGre model is rate dependent. In fact, the input-output maps in Figure 2 show that the LuGre model is rate dependent.

## IV. Hysteresis Induced by Duhem feedback

To study hysteresis induced by Duhem friction models, we consider the feedback interconnection of a SISO linear system and a Duhem hysteretic model as shown in Figure 3. The following definition given in [13] is needed.

*Definition 4.1:* Consider the system in Figure 3 with constant $u$. The system is *step convergent* if $\lim_{t\to\infty} y(t)$ exists for all initial conditions and for all $u \in \mathbb{R}$.

Suppose the feedback system in Figure 3 is step convergent. Then it follows from Definition 4.1 that $\lim_{t\to\infty} y(t)$ exists for every constant $u$. Now, let $u(t) \in [u_{\min}, u_{\max}]$ be

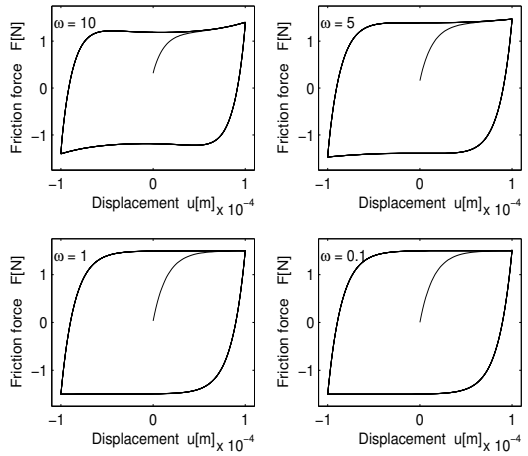


Fig. 2. The input-output maps for the LuGre model. Rate-dependent hysteresis exists between the friction force $F$ and the relative displacement $u$. The numerical values are $F_{\rm C} = 1$ N, $F_{\rm S} = 1.5$ N, $v_{\rm S} = 0.001$ m/s, $\sigma_0 = 10^5$ N/m, $\sigma_1 = \sqrt{10^5}$ N-s/m, $\sigma_2 = 0.4$ N-s/m, and $u(t) = 10^{-4} \sin \omega t$ m.

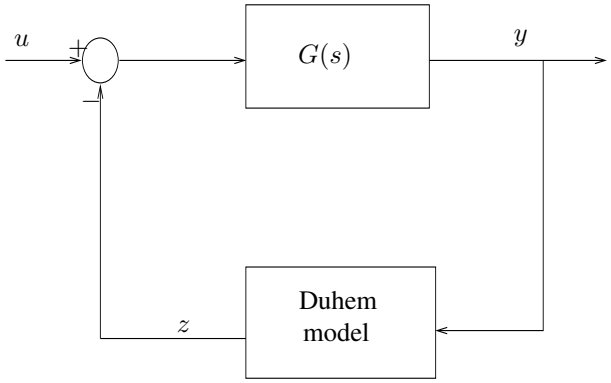


Fig. 3. SISO linear system with Duhem feedback. This model is used to study hysteresis induced by a Duhem friction model when connected by feedback to a linear system.

periodic with period $\alpha$, and let $u_T(t) = u(\alpha t/T)$ for all $t$. Now assume that the periodic input-output map $\mathcal{H}_T(u_T, y_T)$ exists for all $T > 0$ and that the limiting periodic input-output map $\mathcal{H}_\infty(u)$ exists. Since the set $\mathcal{H}_\infty(u)$ represents the response of the feedback system in the limit of dc operation, each element $(u, y)$ of $\mathcal{H}_\infty(u)$ is the limit of a sequence of points $\{(u_i, y_i)\}_{i=1}^{\infty}$, where $(u_i, y_i) \in \mathcal{H}_{T_i}(u_{T_i}, y_{T_i})$ as $T_i \to \infty$, that is, as the input becomes increasingly slower. Since a constant input $u_\infty$ can be viewed as a periodic input with infinite time period, the component $y_\infty$ of each limiting point $(u_\infty, y_\infty) \in \mathcal{H}_\infty(u)$ is given by $y_\infty = \lim_{t\to\infty} y(t)$ under the constant input $u_\infty$. This observation suggests that step convergence of the feedback system is necessary and sufficient for the existence of $\mathcal{H}_\infty(u)$.

Let $\bar{y}_1$ and $\bar{z}_1$ represent limiting values of the outputs of the linear system $G(s)$ and the Duhem model, respectively, for a constant input $u$. If $G(s)$ does not have any poles in the closed right half plane and the system in Figure 3 is step convergent, then

$$\bar{y}_1 = G(0)(u - \bar{z}_1). \tag{23}$$

Now suppose, for some constant $u$, the hysteretic Duhem model has distinct equilibria $\bar{z}_1$ and $\bar{z}_2$. Then the output of the feedback system also has distinct equilibria $\bar{y}_1 = G(0)(u - \bar{z}_1)$ and $\bar{y}_2 = G(0)(u - \bar{z}_2)$. Hence, the limiting periodic map $\mathcal{H}_\infty(u)$ exists, that is, there exists hysteresis between $u(t)$ and $y(t)$. Furthermore, for a given $u$, the horizontal width of the hysteresis map is given by $\bar{y}_1 - \bar{y}_2 = G(0)(\bar{z}_2 - \bar{z}_1)$. In the following section we illustrate these observations with an example.

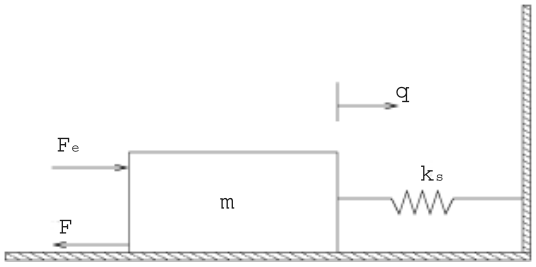


Fig. 4. Force-actuated mass-spring system. The friction force is denoted by $F$ while the external force is $F_{\rm e}$. The system exhibits hysteresis from the external force $F_{\rm e}$ to the displacement $q$ when the Dahl and LuGre models are used to model the friction force $F$.

## V. Hysteresis Induced by Friction in a Mass-Spring System

We now consider the force-actuated mass-spring system shown in Figure 4, whose system dynamics are given by

$$\ddot{q}(t) + \frac{k_{\rm s}}{m} q(t) = \frac{1}{m} F_{\rm e}(t) - \frac{1}{m} F, \tag{24}$$

where $q(t)$ is the displacement of the mass, $k_{\rm s}$ is the spring constant, $m$ is the mass, $F_{\rm e}(t)$ is the external force exerted on the mass, and $F$ is the friction force acting on the mass. Let $v = \dot{q}$ denote the velocity of the mass. This system can be represented as the feedback interconnection of a linear system with a Duhem hysteretic model in Figure 3, where $u = F_{\rm e}$, $y = q$, $z = F$, and the transfer function $G(s)$ is given by

$$G(s) = \frac{1}{ms^2 + k_{\rm s}}. \tag{25}$$

### A. Dahl Model

Using the Dahl model (10) for the friction force with mass displacement $u = q$, we have

$$\dot{F}(t) = \sigma \left| 1 - \frac{F(t)}{F_{\rm C}} \operatorname{sgn} \dot{q}(t) \right|^{\gamma} \operatorname{sgn} \left( 1 - \frac{F(t)}{F_{\rm C}} \operatorname{sgn} \dot{q}(t) \right) \dot{q}(t). \tag{26}$$

As shown above, the friction force given by the Dahl model converges to a constant value $F_{\rm C}$ or $-F_{\rm C}$ depending on the sign of the relative velocity and acts in a direction opposing the motion. Consequently, the Dahl friction acting on the

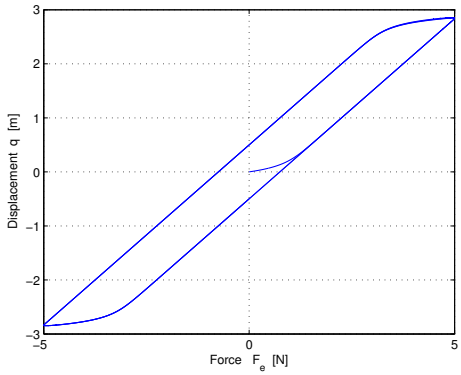


Fig. 5. Hysteresis map from the external force $F_{\rm e}(t)$ to the displacement $q(t)$ of the mass for the force-actuated mass-spring system (24) in Figure 4, with the Dahl model. The numerical values are $F_{\rm C} = 0.75$ N, $\gamma = 1$, $\sigma = 7.5$ N/m, $k_{\rm s} = 1.5$ N/m, $m = 1$ kg, and $F_{\rm e}(t) = 5\sin(0.001t)$ N. The vertical width of the hysteresis map is 1 m.

mass in the mass-spring system plays the role of a damper. Hence, the force-actuated mass-spring system with Dahl friction is step convergent, and the states in the feedback representation (25), (26) converge to constant values for every constant $F_{\rm e} \in \mathbb{R}$. Letting $\bar{q}$, $\bar{v}$, and $\bar{F}$ denote steady-state values, (23), (25), and (26) yield

$$\bar{v} = 0, \tag{27}$$

$$\bar{q} = G(0)(u - \bar{z}) = \frac{F_{\rm e} - \bar{F}}{k_{\rm s}}, \tag{28}$$

$$(1 - \frac{\bar{F}}{F_{\rm C}} \ \text{sgn}\ \bar{v}) = 0. \tag{29}$$

For a constant external force input, the steady-state values of displacement, velocity, and friction force are given by (27), (28), and (29). Thus, for a low-frequency external force input, $v(t) \to 0$, and the displacement of the mass $q(t) \to \bar{q}$, where $\bar{q}$ is given by (28). Now, if (29) holds, then $\bar{F} = F_{\rm C}$ or $\bar{F} = -F_{\rm C}$ depending on the sign of $v(t)$. Consequently, from (28), the steady-state displacement $\bar{q}$ can assume two different values, namely,

$$\bar{q}_1 = G(0)(F_{\rm e} + F_{\rm C}) = \frac{F_{\rm e} + F_{\rm C}}{k_{\rm s}},$$

$$\bar{q}_2 = G(0)(F_{\rm e} - F_{\rm C}) = \frac{F_{\rm e} - F_{\rm C}}{k_{\rm s}}.$$

Hence, the above discussion suggests that the periodic map $\mathcal{H}_T(F_{{\rm e}T}, q_T)$ exists as $T \to \infty$, that is, there exists hysteresis between $F_{\rm e}(t)$ and $q(t)$. The width of the map is given by $\bar{q}_1 - \bar{q}_2 = 2F_{\rm c}/k_{\rm s}$. For $k_{\rm s} = 1.5$ N/m, $F_{\rm c} = 0.75$ N, and $F_{\rm e}(t) = 5\sin(0.001t)$ N, the hysteresis map from the mass displacement $q(t)$ to the external force $F_{\rm e}(t)$ is shown in Figure 5. It can be seen that the vertical width of the hysteresis map is 1 m.

### B. LuGre Model

Using the LuGre model (17), (18) with $u(t) = q(t)$, we have

$$\dot{x}(t) = \dot{q}(t) - \frac{|\dot{q}(t)|}{r\big(\dot{q}(t)\big)}x(t), \tag{30}$$

$$F(t) = \sigma_0 x(t) + \sigma_1 \dot{x}(t) + \sigma_2 \dot{q}(t), \tag{31}$$

where

$$r(\dot{q}(t)) = \frac{F_{\rm C}}{\sigma_0} + \frac{F_{\rm S} - F_{\rm C}}{\sigma_0} e^{-(\dot{q}(t)/v_{\rm S})^2}. \tag{32}$$

Due to the Stribeck effect, relating the equilibria map to the hysteresis map in the case of the LuGre model is more complicated compared to the Dahl model. The friction force acts in a direction opposing the motion and, consequently, plays the role of a damper in the force-actuated mass-spring system. Hence, the force-actuated mass-spring system with LuGre friction is step convergent, and the states in the feedback representation given by (25), (30), and (31) converge to constant values for every constant $F_{\rm e} \in \mathbb{R}$.

The hysteresis map from the input $F_{\rm e}$ to the output $q$ for a low-frequency input $F_{\rm e} = 10\sin(0.001t)$ is shown in Figure 6. The time histories of the friction force $F$ and the position of the mass $q$ are shown in Figure 7. The mass-spring system exhibits stick-slip motion [5] in which the mass sticks until the friction force exceeds the breakaway force $F_{\rm S}$. Once the mass starts moving, the friction force drops because of the Stribeck effect. Consequently, the mass accelerates, and thus the spring contracts and the spring force increases. The mass accelerates until the external force is balanced by the friction force and the spring force. When the spring force becomes sufficiently large, the mass decelerates and sticks again. This process repeats. Stick-slip is reflected by the regions of zero velocity shown in Figure 7(b). The staircase pattern in the hysteresis map shown in Figure 6 is caused by the stick-slip motion. The low-slope horizontal segments of the map correspond to sticking, while the high-slope vertical segments correspond to slip. It should be noted that the hysteresis map is continuous despite the steep vertical segments.

The amplitude of the oscillations in the friction force shown in Figure 7(a) is equal to $F_{\rm S} - F_{\rm C} = 0.5$ N. The length $\Delta F_{\rm e}$ of the horizontal segments of the hysteresis map is twice the amplitude of the oscillations in the friction force, that is, $\Delta F_{\rm e} = 1$ N. The horizontal segments correspond to the sticking phase of the motion, in which the mass is at rest and thus the external force is balanced by the spring force and the friction force. As the external force increases, the friction force also increases until reaching $F_{\rm S}$, after which the mass slips, the friction force drops, and the spring force increases. The larger spring force causes the mass to stick again, leading to new balanced forces.

The vertical segments of the hysteresis map correspond to the slipping phase and their size can be determined by balancing forces. For instance, consider the first vertical step starting from the origin in the hysteresis map. Letting $\Delta q$ be the length of the vertical segment. The external force is

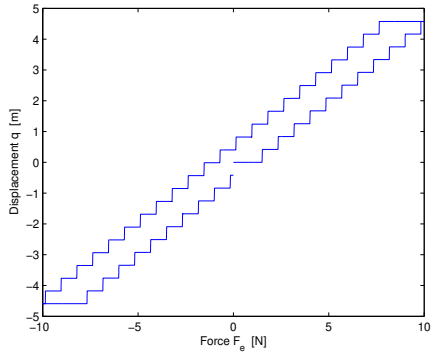


Fig. 6. Hysteresis map from the external force $F_{\rm e}(t)$ to the displacement $q(t)$ of the mass for the force-actuated mass-spring system (24) in Figure 4, with the LuGre model (30),(31). The staircase pattern is caused by the Stribeck effect in the LuGre model. The numerical values are $F_{\rm C} = 1$ N, $F_{\rm S} = 1.5$ N, $v_{\rm S} = 0.001$ m/s, $\sigma_0 = 10^5$ N/m, $\sigma_1 = \sqrt{10^5}$ N-s/m, $\sigma_2 = 0.4$ N-s/m, and $F_{\rm e}(t) = 10\sin(0.001t)$ N.

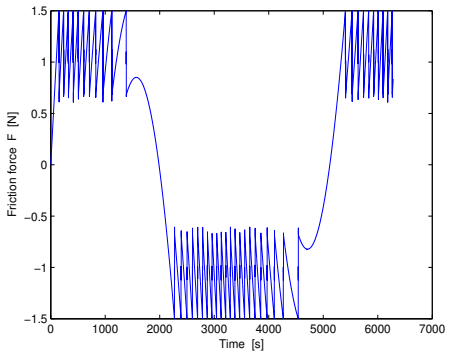


(a)

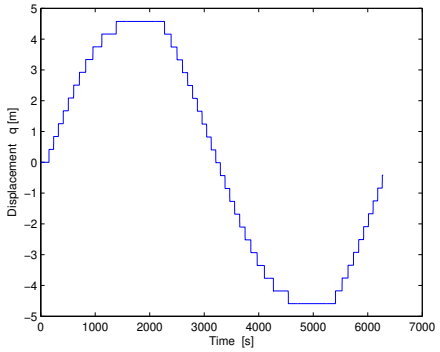


(b)

Fig. 7. (a) Friction force $F(t)$ and (b) displacement $q(t)$ of the mass for the force-actuated mass-spring system (24) in Figure 4, with the LuGre model (30),(31). The friction force oscillates with amplitude $F_{\rm S} - F_{\rm C}$ and the mass exhibits stick-slip motion. The numerical values are $F_{\rm C} = 1$ N, $F_{\rm S} = 1.5$ N, $v_{\rm S} = 0.001$ m/s, $\sigma_0 = 10^5$ N/m, $\sigma_1 = \sqrt{10^5}$ N-s/m, $\sigma_2 = 0.4$ N-s/m, and $F_{\rm e}(t) = 10\sin(0.001t)$ N.

$F_{\rm e} = 1.5$ N and it can be seen in Figure 7(a) that the friction force drops to $F = 0.6$ N, then by balancing the forces, we have the spring force

$$k_{\rm s}\Delta q = F_{\rm e} - F = 1.5 - 0.6 = 0.9 \ \ {\rm N},$$

which implies that

$$\Delta q = \frac{0.9}{k_{\rm s}} = \frac{0.9}{2} = 0.45 \ \ {\rm m}.$$

Thus the hysteresis map can be completely determined in terms of the parameters $F_{\rm S}$, $F_{\rm C}$, $m$, and $k_{\rm s}$.

## VI. Conclusion

In this paper we have studied the hysteresis induced by a Duhem feedback in a SISO linear system. Then, we modeled the mass-spring system with friction as a linear system with a Duhem feedback. We used the feedback model to study the hysteresis between the external force excitation and the position of the mass. We showed that the hysteresis map can be completely characterized in terms of the parameters used in the friction model and the mass-spring system. With the LuGre model the hysteresis map has a unique staircase pattern. The staircase pattern occurs because of the stick-slip motion which in turn is caused by the Stribeck effect in the LuGre model.

## References


[1] B. Armstrong-Hélouvry, *Control of Machines with Friction*. Boston, MA: Kluwer, 1991.

[2] B. Armstrong-Hélouvry, P. Dupont, and C. C. de Wit, "A survey of model, analysis tools and compensation methods for the control of machines with friction," *Automatica*, vol. 30, no. 7, pp. 1083–1138, 1994.

[3] B. Feeny, A. Guran, N. Hinrichs, and K. Popp, "Historical review on dry friction and stick-slip phenomena," *Applied Mechanics Reviews*, vol. 51, no. 5, pp. 321–341, 1998.

[4] P. Dahl, "Solid friction damping of mechanical vibrations," *AIAA J.*, vol. 14, no. 2, pp. 1675–82, 1976.

[5] C. Canudas de Wit, H. Olsson, K. J. Åstrom, and P. Lischinsky, "A new model for control of systems with friction," *TAC*, vol. 40, no. 3, pp. 419–425, 1995.

[6] D. D. Rizos and S. D. Fassois, "Presliding friction identification based upon the Maxwell slip model structure," *Chaos*, vol. 14, no. 2, pp. 431–445, 2004.

[7] F. Al-Bender, V. Lampaert, and J. Swevers, "Modeling of dry sliding friction dynamics: From heuristic models to physically motivated models and back," *Chaos*, vol. 14, no. 2, pp. 446–445, 2004.

[8] F. Al-Bender, V. Lampaert, S. D. Fassois, D. D. Rizos, K. Worden, D. Engster, A. Hornstein, and U. Parlitz, "Measurement and identification of pre-sliding friction dynamics," in *Nonlinear Dynamics of Production Systems*. Weinheim: Wiley, 2004, pp. 349–367.

[9] J. Oh, A. Padthe, D. S. Bernstein, D. D. Rizos, and S. D. Fassois, "Duhem models for hysteresis in sliding and presliding friction," in *Proc. IEEE Conf. Dec. Contr.*, Seville, Spain, December 2005, pp. 8132–8137.

[10] J. Oh and D. S. Bernstein, "Semilinear Duhem model for rate-independent and rate-dependent hysteresis," *IEEE Trans. Autom. Contr.*, vol. 50, no. 5, pp. 631–645, 2005.

[11] A. Padthe, J. Oh, and D. S. Bernstein, "On the lugre model and friction-induced hysteresis," in *Proc. Amer. Contr. Conf.*, Minneapolis, MN, June 2006.

[12] J. Swevers, F. Al-Bender, C. G. Ganseman, and T. Prajogo, "An integrated friction model structure with improved presliding behavior for accurate friction compensation," *IEEE Trans. Autom. Contr.*, vol. 45, no. 4, pp. 675–686, 2000.

[13] S. L. Lacy, D. S. Bernstein, and S. P. Bhat, "Hysteretic systems and step-convergent semistability," in *Proc. Amer. Contr. Conf.*, Chicago, IL, June 2000, pp. 4139–4143.